


PRIMARY RESEARCH ARTICLE

WILEY Global Change Biology

Rapid thermal adaptation in a marine diatom reveals constraints and trade-offs

Daniel R. O'Donnell^{1,2,3}  | Carolyn R. Hamman¹ | Evan C. Johnson¹ |
Colin T. Kremer^{1,4} | Christopher A. Klausmeier^{1,3,4} | Elena Litchman^{1,2,3}

¹W. K. Kellogg Biological Station, Michigan State University, Hickory Corners, Michigan

²Department of Integrative Biology, Michigan State University, East Lansing, Michigan

³Program in Ecology, Evolutionary Biology and Behavior, Michigan State University, East Lansing, Michigan

⁴Department of Plant Biology, Michigan State University, East Lansing, Michigan

Correspondence

Daniel R. O'Donnell, W. K. Kellogg Biological Station, Michigan State University, 3700 E. Gull Lake Dr., Hickory Corners, MI 49060.
Email: odonn146@msu.edu

Funding information

National Science Foundation, Grant/Award Number: OCE 0928819, OCE 1638958

Abstract

Rapid evolution in response to environmental change will likely be a driving force determining the distribution of species across the biosphere in coming decades. This is especially true of microorganisms, many of which may evolve in step with warming, including phytoplankton, the diverse photosynthetic microbes forming the foundation of most aquatic food webs. Here we tested the capacity of a globally important, model marine diatom *Thalassiosira pseudonana*, for rapid evolution in response to temperature. Selection at 16 and 31°C for 350 generations led to significant divergence in several temperature response traits, demonstrating local adaptation and the existence of trade-offs associated with adaptation to different temperatures. In contrast, competitive ability for nitrogen (commonly limiting in marine systems), measured after 450 generations of temperature selection, did not diverge in a systematic way between temperatures. This study shows how rapid thermal adaptation affects key temperature and nutrient traits and, thus, a population's long-term physiological, ecological, and biogeographic response to climate change.

KEYWORDS

experimental evolution, function-valued trait, nitrate growth affinity, temperature optimum, *Thalassiosira pseudonana*, thermal reaction norm, trade-off

1 | INTRODUCTION

The dependence of physiological processes on temperature is perhaps the most important factor determining the fitness of organisms across latitudinal and altitudinal gradients, and thus their distributions and abundances on Earth. Due to climate warming, many studies have focused on the temperature dependence of physiological traits (e.g., photosynthesis, respiration, per-capita population growth) near the upper bounds of organisms' thermal tolerance ranges (Bradford, 2013; Listmann, LeRoch, Schlüter, Thomas, & Reusch, 2016; Rowan, 2004) and the ecological consequences of temperatures rising beyond those ranges (Bradford, 2013; Listmann et al., 2016; Rowan, 2004; Thomas, Kremer, Klausmeier, & Litchman, 2012). Studies have increasingly focused on the potential for rapid evolution of traits in response to temperature change, and how such evolution

may mitigate the ecological impacts of climate warming (Hoffmann & Sgrò, 2011; Listmann et al., 2016; Schlüter et al., 2014).

Evolution on ecological timescales may be commonplace (Schoener, 2011) and can “rescue” populations from potentially catastrophic environmental change (Bell, 2013; Gomulkiewicz & Holt, 1995; Schiffrs, Bourne, Lavergne, Thuiller, & Travis, 2013). In particular, the enormous population sizes and fast reproduction of microorganisms, on the order of hours to days, offer many opportunities for rapid evolution in response to environmental change. Phytoplankton are a diverse and often overlooked microbial group of global importance: they are the foundation of most marine and freshwater food webs and are major drivers of global biogeochemical cycles, carrying out ~50% of global carbon fixation (Field, Behrenfeld, Randerson, & Falkowski, 1998) and linking nitrogen and phosphorus

cycles (Redfield, 1958). Rising temperatures may negatively impact phytoplankton productivity, biomass and species diversity (Boyce, Lewis, & Worm, 2010; Thomas et al., 2012). However, rapid adaptation to warming may mitigate some ecological impacts of climate change (Listmann et al., 2016; Litchman, Edwards, Klausmeier, & Thomas, 2012). For example, evolutionary change in the thermal optimum for per-capita population growth (T_{opt}) and the maximum temperature at which positive growth is possible (CT_{max}) in response to ocean warming may reduce heat-induced mortality, allowing some species to persist at low latitudes where they might otherwise go regionally extinct (Thomas et al., 2012).

A number of recent evolution experiments have investigated how marine phytoplankton may evolve to cope with environmental change (Reusch & Boyd, 2013), though most have focused only on increased atmospheric $p\text{CO}_2$ and/or ocean acidification (Crawford, Raven, Wheeler, Baxter, & Joint, 2011; Jin, Gao, & Beardall, 2013; Lohbeck, Riebesell, & Reusch, 2012). Thermal adaptation has been studied experimentally in only a couple of phytoplankton species, only one of which, a coccolithophorid, was a marine species of global importance (Listmann et al., 2016; Padfield, Yvon-Durocher, Buckling, Jennings, & Yvon-Durocher, 2015; Schlüter et al., 2014). It is therefore difficult to predict if other ecologically important groups, such as diatoms that contribute up to 25% of all global carbon fixation (Nelson, Tréguer, Brzezinski, Leynaert, & Quéguiner, 1995), would respond similarly. Moreover, while we may expect T_{opt} and CT_{max} to increase after evolving at high temperatures (Listmann et al., 2016; Schaum et al., 2017), knowledge of how other important traits may change in response to elevated temperatures is limited, though some significant work has been done on rapid temperature-dependent evolution of metabolic traits in freshwater chlorophytes (Padfield et al., 2015; Schaum et al., 2017). Schlüter et al. (2014) found that after 1 year of experimental adaptation to elevated temperature (26.3°C), the marine coccolithophore *Emiliania huxleyi* evolved a higher population growth rate, smaller cell diameter and lower particulate organic and inorganic carbon content compared to cold (15°C)-adapted populations. Hinnert, Kremp, and Hense (2017) found that 100-year-old resurrected strains of the marine dinoflagellate *Apocalathium malmogiense* did not differ in cell size or in its thermal reaction norm for growth compared to current strains, but that it did form resting cysts at a higher rate.

Large-scale evolutionary change in nutrient utilization traits in response to changing climate could significantly impact biogeochemical cycling (Field et al., 1998). A number of studies have examined the interactive effects of temperature and nutrient on per-capita population growth rates in phytoplankton (Thomas et al., 2017; Tilman, Mattson, & Langer, 1981), and some have tested the effects of temperature on elemental (C, N, P) stoichiometry. Martiny, Ma, Mouginot, Chandler, and Zinser (2016) studied temperature effects on growth and elemental stoichiometry in several *Prochlorococcus* species, but did not find consistent trends across closely related species, suggesting that effects of thermal adaptation on nutrient utilization traits are idiosyncratic and not necessarily consistent; Thrane, Hessen, and Anderson (2017) conducted a large, factorial experiment

to elucidate the effect of temperature on optimal N:P supply ratio in the freshwater chlorophyte *Chlamydomonas reinhardtii*; and Yvon-Durocher, Schaum, and Trimmer (2017) studied temperature effects on seston stoichiometry in a mesocosm community, emphasizing long-term evolutionary effects on cellular stoichiometry, also in *C. reinhardtii*. However, this study is novel in that it directly tests whether a key measure of competitive ability for nitrate, nitrate growth affinity, evolves in distinct temperature environments in the model marine diatom *Thalassiosira pseudonana*.

Biological rates in ectotherms vary continuously across temperature and are, thus, often referred to as “function-valued traits” (Kingsolver, Gomulkiewicz, & Carter, 2001). Our understanding of how diverse function-valued traits may evolve in different organisms is limited. Trade-offs (e.g., generalist-specialist or resource allocation trade-offs) may be important in determining how the shapes of trait functions, including the thermal reaction norm, evolve (Angilletta, Wilson, Navas, & James, 2003). The trait values derived from thermal reaction norms and many other function-valued traits are nonindependent across temperature gradients (Angilletta et al., 2003); thus, selection at one temperature may alter rates (e.g., population growth rate) at every other temperature along the thermal reaction norm. The underlying mechanisms of thermal adaptation and its associated trade-offs may lie in any of myriad of metabolic and physiological pathways within the organism. For example, allocation of resources to constitutive adaptations to cold environments may preclude those resources from being used to synthesize heat shock proteins when the environment unexpectedly warms; nitrate uptake machinery optimized for warm environments may not function well in cold environments; membrane lipids may be comprised of many highly unsaturated fatty acids in a cold-adapted organism, but such fatty acids lead to excessive membrane fluidity in a warm environment (Jiang & Gao, 2004); or, in any of these cases, plasticity in traits (i.e., in a generalist) may lower the maximum achievable functionality of each trait at every temperature (a generalist–specialist trade-off).

While recent studies showed that T_{opt} and CT_{max} increase after evolving at higher temperatures (Listmann et al., 2016), we do not know how the whole thermal reaction norm may evolve in phytoplankton; for example, adaptation to high temperatures may lead to a decrease in fitness at low temperatures, as previously observed in bacteria (Bennett & Lenski, 1993) and bacteriophages (Knies, Izem, Supler, Kingsolver, & Burch, 2006). Selection may change the slope and curvature (first and second derivatives) of the thermal reaction norm as well (Kutcherov, 2016), especially if some cardinal temperatures are more evolutionarily labile than others (Araújo et al., 2013). For example, by comparing the peak sharpness at T_{opt} and the width (°C) of the upper tail of the thermal reaction norm in cold- versus warm-selected populations, we may make inferences regarding the evolutionary lability of the maximum growth rate at T_{opt} (μ_{opt}), and of T_{opt} itself, relative to that of CT_{max} ; the upward concavity below T_{opt} and the location of the inflection point on the thermal reaction norm contribute greatly to the magnitude of trade-offs between growth at temperatures below T_{opt} versus above, which can be

indicative of generalist-specialist and/or resource allocation trade-offs (Angilletta et al., 2003; Gilchrist, 1995).

The thermal reaction norm for population growth depends on the temperature dependences of enzyme activities (Corkrey et al., 2014; Ratkowsky, Olley, & Ross, 2005), and few processes or pathways within the cell should be immune to the effects of directional temperature selection (Baker et al., 2016; Nedwell, 1999; Padfield et al., 2015; Schaum et al., 2017). Depending on the genes affected, changes in growth rate may be accompanied by changes in traits not directly associated with the thermal reaction norm. For example, stoichiometry may respond to thermal adaptation due to changes in relative resource requirements of phytoplankton cells, which in turn may affect species' competitive abilities (e.g., for N and P) and ultimately global biogeochemical cycles (Baker et al., 2016; Litchman, Klausmeier, Schofield, & Falkowski, 2007; Redfield, 1958). An increase in maximum growth rate at the selection temperature may lead to a decrease in affinity for a given nutrient due to a trade-off between allocation of cellular resources to reproduction versus nutrient uptake (Grover, 1991; Klausmeier, Litchman, Daufresne, & Levin, 2004). If the nutrient in question is never limiting, selection may favor a high maximum growth rate over affinity, and the trade-off may ultimately result in a weakening of competitive ability for that nutrient in the selection environment. Moreover, adaptation to high temperature may require higher investment in repair machinery, such as heat shock proteins, potentially increasing the demand for nitrogen and other nutrients.

Here, we performed a 350-generation selection experiment on a model marine diatom, *Thalassiosira pseudonana*, to determine whether and how its thermal performance curves evolve and diverge under selection at two different temperatures, above and below the growth optimum, and whether other key traits, such as nitrate utilization traits, evolve as well. Postselection, we conducted temperature and nutrient-dependent growth assays to assess evolutionary divergence in temperature and nutrient traits resulting from thermal adaptation.

2 | MATERIALS AND METHODS

2.1 | Temperature selection experiment

We obtained a monoculture of *Thalassiosira pseudonana* CCMP1335 (Hustedt) Hasle et Heimdal from the Provasoli-Guillard National Center for Culture of Marine Phytoplankton (CCMP), Maine, USA, and isolated a single cell by plating on agarose ESAW marine culture medium (Harrison, Waters, & Taylor, 1980). Nitrogen (as NaNO_3), phosphorus (as $\text{NaH}_2\text{PO}_4 \cdot \text{H}_2\text{O}$), and silicon (as $\text{NaSiO}_3 \cdot 9\text{H}_2\text{O}$) concentrations were 549, 22.4, and 106 $\mu\text{mol/L}$, respectively. We cultured the resulting colony in a flask of ESAW medium until it reached a high density. "Generation zero" was on April 14, 2014, when we propagated 10 replicate populations from the progenitor culture ("selection lines" hereafter) into 20 ml ESAW medium in 50 ml Cellstar polystyrene tissue culture flasks with breathable caps (Greiner Bio-One GmbH, Frickenhausen, Germany), which we gently

agitated daily to keep cells in suspension. We assigned five replicates to the 16°C treatment and the other five to 31°C. These two temperatures were below and above the previously recorded thermal optimum (T_{opt}) of *T. pseudonana* (between 24 and 26°C) (Boyd et al., 2013) under similar culture conditions. We chose these selection temperatures so that the maximum growth rates (μ_{max}) at the two temperatures were roughly equal ($\sim 0.8/\text{day}$ at the start of the experiment). The low temperature treatment was close to the ancestral maintenance temperature of 14°C (see technical specifications on CCMP1335 culture maintenance at <https://ncma.bigelow.org/catalogsearch/result/?q=1335>) and 16°C was thus used for the main comparison of the evolution in response to different temperatures. Such a comparison allows isolation of the selection effect of temperature itself from the effect of the cultivation regime, as both temperature treatments experience the same maintenance for the duration of the experiment. In contrast, the common comparison in many experimental evolution studies of the treatment and the ancestral strain that did not experience the same selection regime may confound the effect of the focal selection force and the culturing conditions.

Selection lines were maintained in temperature-controlled growth chambers at 110 $\mu\text{mol photons m}^{-2} \text{ s}^{-1}$ under a 14:10 light:dark cycle (note that this is 10 $\mu\text{mol photons m}^{-2} \text{ s}^{-1}$ higher than the light level in Boyd et al. (2013), but still in the saturating range). All lines were maintained in ESAW medium for ~ 50 generations at a dilution rate of 0.5/day (diluted daily), after which (August 12, 2014) all cultures were transferred to L1 medium (Guillard & Hargraves, 1993) due to poor culture health in ESAW. L1 was made using 43.465 g/l artificial sea salt (Tropic Marin, Wartenberg, Germany), which yields a specific gravity of 1.025, similar to natural seawater, with NaNO_3 , $\text{NaH}_2\text{PO}_4 \cdot \text{H}_2\text{O}$, and $\text{NaSiO}_3 \cdot 9\text{H}_2\text{O}$ concentrations of 882, 36.3, and 107 $\mu\text{mol/L}$, respectively. Upon switching culture media, we also altered the dilution regime, such that 10^6 cells (usually $\sim 0.5\text{--}1.0 \text{ ml}$) were transferred to fresh medium every 4 days (with occasional deviations of ± 1 day). The selection lines required an additional ~ 50 generations to adjust to the new dilution regime before consistent growth rates and culture health were achieved. These changes led to a substantial reduction in the variability of growth rates over time. Cell densities of all replicate cultures were determined at each transfer for the remainder of the experiment using a CASY particle counter (Schärfe System GmbH, Reutlingen, Germany), and average population growth rates for each propagation period determined by taking $\log(N_t/N_0)/t$, where N is the population density and t is time in days.

2.2 | Determination of postselection physiological trait values

2.2.1 | Temperature-dependent growth assays

To evaluate evolutionary change in thermal reaction norms after ~ 350 generations, we conducted temperature-dependent population growth assays on evolved selection lines. First, we subcultured all

selection lines and acclimated subcultures to 10 temperatures spanning the thermal niche for ~12 generations (days to acclimation ranged from ~10 days at near-optimal temperatures to more than a month at 3°C). Approximately 10^5 cells from each acclimated culture were then propagated into an identical flask containing fresh L1 medium, and the cell density was estimated daily at the acclimated temperature until stationary phase (5–10 days, depending on the temperature). Light conditions were as above. Culture density was estimated daily at all temperatures $\geq 16^\circ\text{C}$ by placing the polystyrene culture flask in a Shimadzu UV-2401PC spectrophotometer (Shimadzu Corporation, Kyoto, Japan) and measuring Abs_{436} (the wavelength corresponding to the absorbance maximum of chlorophyll *a*: Neori, Vernet, Holm-Hansen, & Haxo, 1986). At 3 and 10°C , due to fogging of culture flasks, daily density estimates were conducted using the CASY counter instead; to make sure density estimation method did not bias estimates, we checked model residuals at 3 and 10°C against those from other temperatures, and found no indication of method-induced bias (see Supporting Information Figure S1). We calculated exponential growth rates by fitting regression lines to log-transformed population densities over time; with a minimum of three points that best represented exponential-phase growth (those that formed a straight line when log-transformed). Single cultures of each selection line were assayed at each temperature, except those at 16 and 31°C , which were assayed in triplicate to facilitate direct statistical comparison of growth rates ($n = 14$ total points per thermal reaction norm). This comparison serves as a “reciprocal transplant” experiment, a common approach to test for local adaptation (Blanquart, Kaltz, Nuismer, & Gandon, 2013; Kawecki & Ebert, 2004).

We derived temperature-dependent trait values by fitting a model proposed by Logan, Wollkind, Hoyt, and Tanigoshi (1976) and recently used by Thomas et al. (2017), in which birth and death are both exponential functions of temperature. The resulting curve is a unimodal, left-skewed thermal reaction norm. In the following double-exponential equation, the first term is the exponential birth term, the second term is the exponential mortality term:

$$\mu_{\max} = b_1 e^{b_2 T} - d_1 e^{d_2 T} - d_0 \quad (1)$$

where μ_{\max} is the specific growth rate (day^{-1}), T is temperature, b_1 and d_1 are the pre-exponential constants for birth and death, respectively, b_2 and d_2 are the exponential rates of increase in both terms, and d_0 is the temperature-independent death rate. To facilitate fitting this model, we used an alternative parameterization of 1 that includes an explicit T_{opt} parameter, thus making it possible to directly compute 95% confidence intervals for this trait (see Supporting information Appendix A); the two formulations are mathematically equivalent and yield similar fits. We determined the “sharpness” of the thermal reaction norm peaks by taking the second derivative of the thermal reaction norm with respect to temperature at T_{opt} (“Peak sharpness” [Figure 3b] is the negative of this number), and the upward concavity below T_{opt} by computing the maxima in the second derivative across $0 \leq T \leq T_{\text{opt}}$. We estimated the inflection point of each thermal

reaction norm by setting $\frac{\partial^2 \mu_{\max}}{\partial T^2} = 0$ and solving for T within the range $0 \leq T \leq T_{\text{opt}}$.

2.3 | Nitrate-dependent growth assays

Per-capita population growth as a function of external nitrate concentration can be described using the Monod equation (Monod, 1949):

$$\frac{1}{N} \frac{dN}{dt} = \frac{\mu_{\max} a R}{\mu_{\max} + a R} \quad (2)$$

where N is the population density, R is the resource (nitrate) concentration, μ_{\max} is the resource-saturated (maximum) population growth rate, and a ($\text{L } \mu\text{mol}^{-1} \text{ day}^{-1}$) is the nitrate growth affinity (the initial slope of the Monod curve). Note that this formulation directly incorporates the affinity a , rather than the traditional formulation with the half-saturation constant for growth, K . Growth affinity is a more mechanistic parameter because it is more directly indicative of competitive ability (Healy, 1980). The two parameters are related by $K = \mu_{\max}/a$. For a full derivation of Equation 2, see Supporting information Appendix A.

To determine if the nutrient-related traits changed as a result of adaptation to different temperatures, we estimated Monod growth curves for nitrate at 16 and 31°C after ~450 generations. The difference in the number of generations elapsed for the temperature and nutrient trait assays was due to the logistical infeasibility of running those experiments simultaneously. We investigated whether temperature selection had caused evolutionary divergence in nitrate growth affinities between lines from each temperature treatment when assayed at both selection temperatures, and whether this divergence corresponded to the trade-off between the maximum growth rate and nitrate growth affinity. Selection lines were assayed in triplicate at each selection temperature and at ten nitrate concentrations (0, 2.5, 5, 10, 20, 40, 60, 90, 180 and $882 \mu\text{mol/L}$), the latter being the N concentration of undiluted L1 medium). Prior to the Monod assay, all lines were acclimated to assay temperatures as above, followed by a 5-day N-starvation period in which cultures were kept in modified N-free L1 medium. Population growth rates were estimated as for temperature-dependent growth assays. In some replicates, an opaque, white contaminant was visible, which appeared under the microscope to be bacteria; these replicates were excluded from analyses.

2.4 | Model fitting, trait estimation, and statistical analysis

We conducted all statistical analyses using R statistical programming language, version 3.3.2. We fit Equation 1 to temperature-dependent growth data using the “mle2()” function from the “bbmle” package (Bolker, 2017). Due to high uncertainty in some growth rate estimates in Monod assays, we used weighted, nonlinear least squares regression to fit Equation 2 to nutrient-dependent growth data, weighting growth rate estimates by their inverse variances.

We compared traits derived from thermal reaction norms by conducting ANOVA on weighted least squares linear models. To quantify uncertainty in all trait estimates (except T_{opt}) for each selection line, we conducted 1,000 residual bootstraps of the double-exponential fits using a procedure described in Listmann et al. (2016). We incorporated this uncertainty into linear models by weighting each trait estimate for each selection line by the inverse of the variance of its bootstrap distribution (see Supporting information Model S1), except in the case of T_{opt} , where we were able to directly employ its variance, though T_{opt} variances estimated directly were nearly identical to those estimated via bootstrapping (Supporting information Figure S3).

We used a nested ANOVA to compare maximum growth rates (μ_{max}) at the selection temperatures in a reciprocal transplant (all 16°C- and 31°C-selected lines assayed at both temperatures). Uncertainty in μ_{max} could be estimated directly ($n = 3$, no bootstraps), and we fit a *selection temperature* \times *assay temperature* interaction and nested replicate selection line within selection temperature to test for local adaptation and strain-level selection temperature effects, respectively (Supporting information Model S2).

We compared μ_{max} and nitrate growth affinity (a_{NO3}) estimates derived from fits of the Monod equation to growth rates estimated across a nitrate gradient at the selection temperatures (reciprocal transplant scenario) using two-way ANOVA conducted on weighted, least squares linear models (Supporting information Equation S3), as above. Uncertainties in these trait estimates were estimated directly when fitting the Monod equation, as its parameters are the traits being compared; uncertainties were incorporated into the linear model as weights ($(1/\sigma^2)$), as was done with bootstrap variances above. To test for a global trade-off between μ_{max} and a_{NO3} within selection groups (pooled across assay temperatures), we used Deming regression, a form of orthogonal regression that allows for uncertainty in individual measurements and assumes unequal variances in x and y . We conducted this test using the “mcreg()” function in the “mcr” package in R (Manuilova, Schuetzenmeister, & Model, 2014). Note in the results below that we did not obtain t -statistics or p -values from the Deming regression, but that we used a bootstrapping option built into the mcreg() function to calculate 95% confidence intervals for slopes and intercepts. All data files and R code used in this study are included in the supporting information.

3 | RESULTS

3.1 | Evolutionary change in thermal reaction norms

Growth for 350 generations at two different temperatures, below and above the temperature optimum for *T. pseudonana* (16 and 31°C), led to a significant divergence of the thermal reaction norms (Figure 1). T_{opt} was 1.87°C higher, on average, in selection lines evolved at 31°C than in those evolved at 16°C ($F_{1,8} = 17.02$; $p = 0.0033$; Figure 2a; Supporting information Table S1); the maximum growth rate at T_{opt} (μ_{opt}) was also $\sim 0.1/\text{day}$ higher in 31°C-

selected lines ($F_{1,8} = 7.99$; $p = 0.022$; Figure 2b; Supporting information Table S1). CT_{max} trended higher in 31°C-selected lines than in 16°C-selected lines, with one exception (replicate line 31_5), though the difference was not statistically significant ($F_{1,8} = 2.09$; $p = 0.19$; Figure 2c; Supporting information Table S1).

A “reciprocal transplant” comparison between temperature treatments revealed that selection lines from each treatment had higher maximum growth rates (μ_{max}) in their “home” temperature environments than in “away” environments; “local” lines also had higher growth rates than “foreign” lines (*assay temp.* \times *selection temp.* interaction: $F_{1,8} = 254.82$; $p < 0.0001$; Figure 2d; Supporting information Table S1; see Supporting information Figure S2 for population-level effects). Taken together, these results are the signature of local adaptation to temperature (Blanquart et al., 2013; Kawecki & Ebert, 2004). While μ_{max} estimates differed slightly between 350 and 450 generations (measured for thermal reaction norm and Monod assays, respectively), differences were not directionally consistent across selection lines, and the overall pattern of local adaptation persisted (see next section; Supporting information Figure S5a; Supporting information Table S3).

The peaks of the thermal reaction norms of 31°C-selected lines appeared sharper, and the left tails more deeply concave-up than those of 16°C-selected lines, both for the parametric (Figure 1) and nonparametric (Supporting information Figure S6) thermal reaction norms. These observations, combined with the statistically nonsignificant difference in CT_{max} between the two selection regimes, led us to hypothesize that CT_{max} is less evolutionarily labile than T_{opt} , resulting in greater skew in thermal reaction norms of 31°C-selected lines, rather than a simple rightward shift of the thermal reaction norms along the temperature axis. The difficulty in reliably estimating CT_{min} prevented statistical

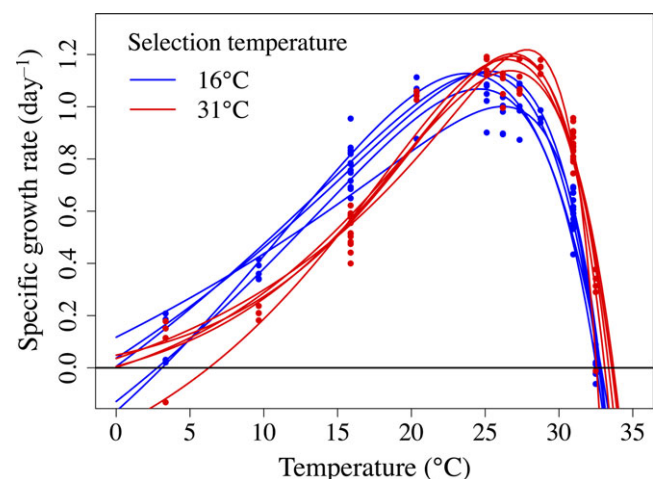


FIGURE 1 Thermal reaction norms for per-capita population growth of 10 *Thalassiosira pseudonana* populations. Growth rates were measured at 10 temperatures for each replicate population (five selected at 16°C [red] and five selected at 31°C [blue]) after 350 generations of experimental selection. Growth rates were measured in triplicate at the selection temperatures (reciprocal transplant scenario). $N = 14$ for each curve

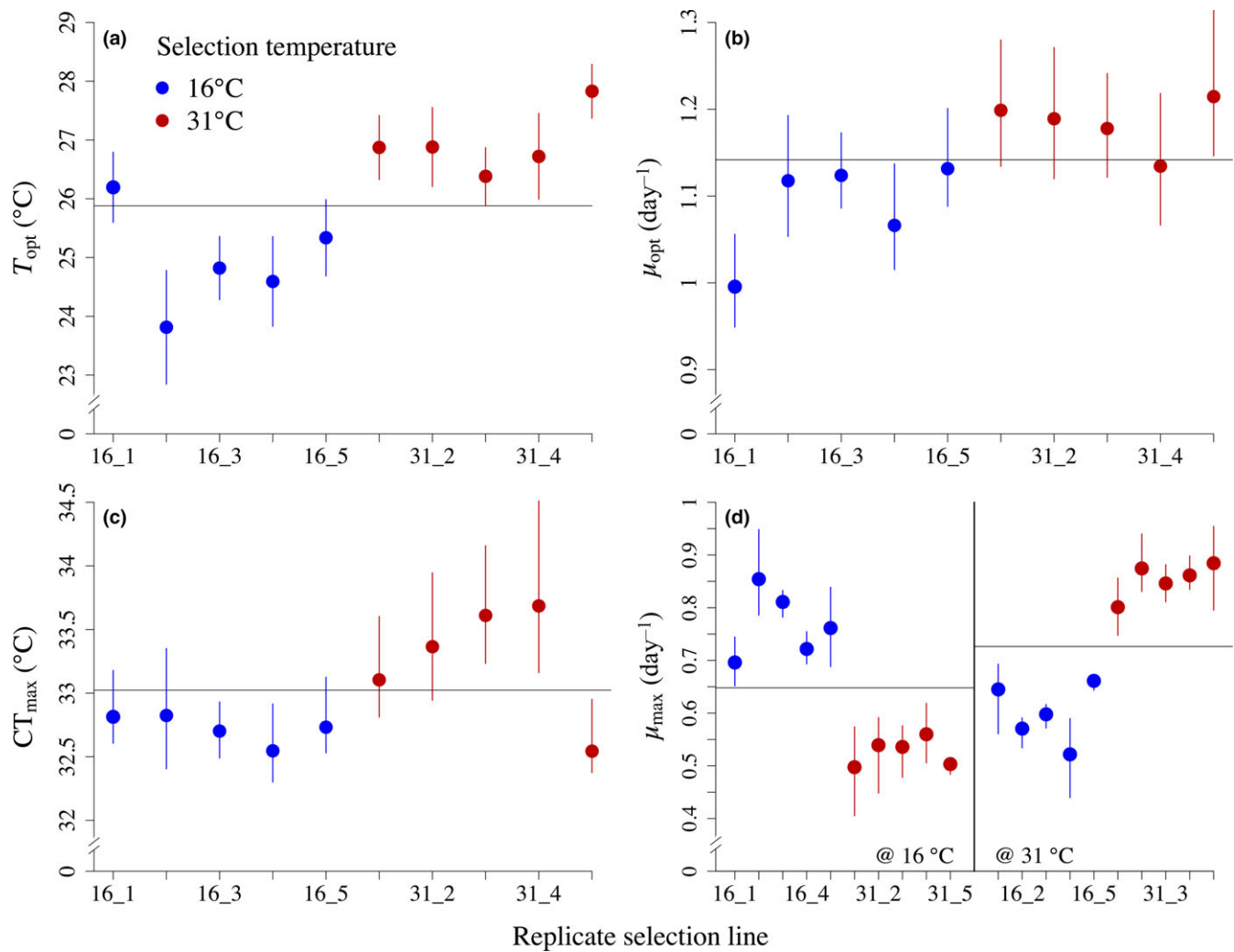


FIGURE 2 Thermal performance traits of 16°C- and 31°C-selected populations. I. (a) Thermal optimum (T_{opt}); (b) Maximum growth rates at T_{opt} (μ_{opt}); (c) Upper critical temperature (CT_{max}); (d) μ_{max} at the selection temperatures in the reciprocal transplant scenario (both selection groups assayed at both selection temperatures). All trait estimates in (b–c) were derived numerically from fits of the double-exponential model. Bars in (a) are Fisher's 95% CI estimated directly from the standard errors of double-exponential T_{opt} parameter estimates. Bars in (b–c) are 95% CI estimated as 2.5%–97.5% quantiles of bootstrap distributions ($n = 1,000$ bootstraps for each replicate population); bars in (d) are 95% CI directly from triplicate growth rate estimates (no bootstrapping). In (a–c), the horizontal line across the whole panel is the grand mean across trait estimates for all replicate populations; in (d), horizontal lines are grand means for assay temperature groups

comparisons of CT_{min} and of thermal niche width among selection lines, and also prevented estimation of skewness. However, we determined the distance between T_{opt} and CT_{max} for all bootstrapped thermal reaction norms; ideally, this distance would be scaled by thermal niche width, but absence of reliable thermal niche width estimates prevented scaling. The distance between T_{opt} and CT_{max} ("upper tail length") was smaller in 31°C-selected lines than in 16°C-selected lines ($F_{1,8} = 6.58$; $p = 0.033$; Figure 3a; Supporting information Table S2), suggesting that the change in T_{opt} was greater than the change in CT_{max} at one or, possibly, both selection temperatures. The 31°C-selected lines had sharper peaks at T_{opt} ($F_{1,8} = 26.77$; $p = 0.00085$; Figure 3b; Supporting information Table S2), were more deeply concave-up below T_{opt} ($F_{1,8} = 91.41$; $p < 0.0001$; Figure 3c; Supporting information Table S2), and had inflection points at higher temperatures than

16°C-selected lines ($F_{1,8} = 12.36$; $p = 0.0079$; Figure 3d; Supporting information Table S2), suggesting greater negative skew.

3.2 | Evolution of competitive ability for nitrate

Temperature selection did not lead to consistent evolutionary divergence in competitive ability for nitrate; there was no significant effect of assay temperature ($F_{1,16} = 0.27$; $p = 0.61$) or selection temperature ($F_{1,16} = 1.26$; $p = 0.28$) on nitrate growth affinity (a_{NO_3}), nor was there an assay temperature \times selection temperature interaction ($F_{1,16} = 0.12$; $p = 0.74$; Supporting information Table S3; Supporting information Figures S4 and S5). The differences in a_{NO_3} among selection groups or assay temperatures appeared idiosyncratic, with estimates ranging over nearly an order of magnitude across replicate populations. However, as in the reciprocal transplant above, there

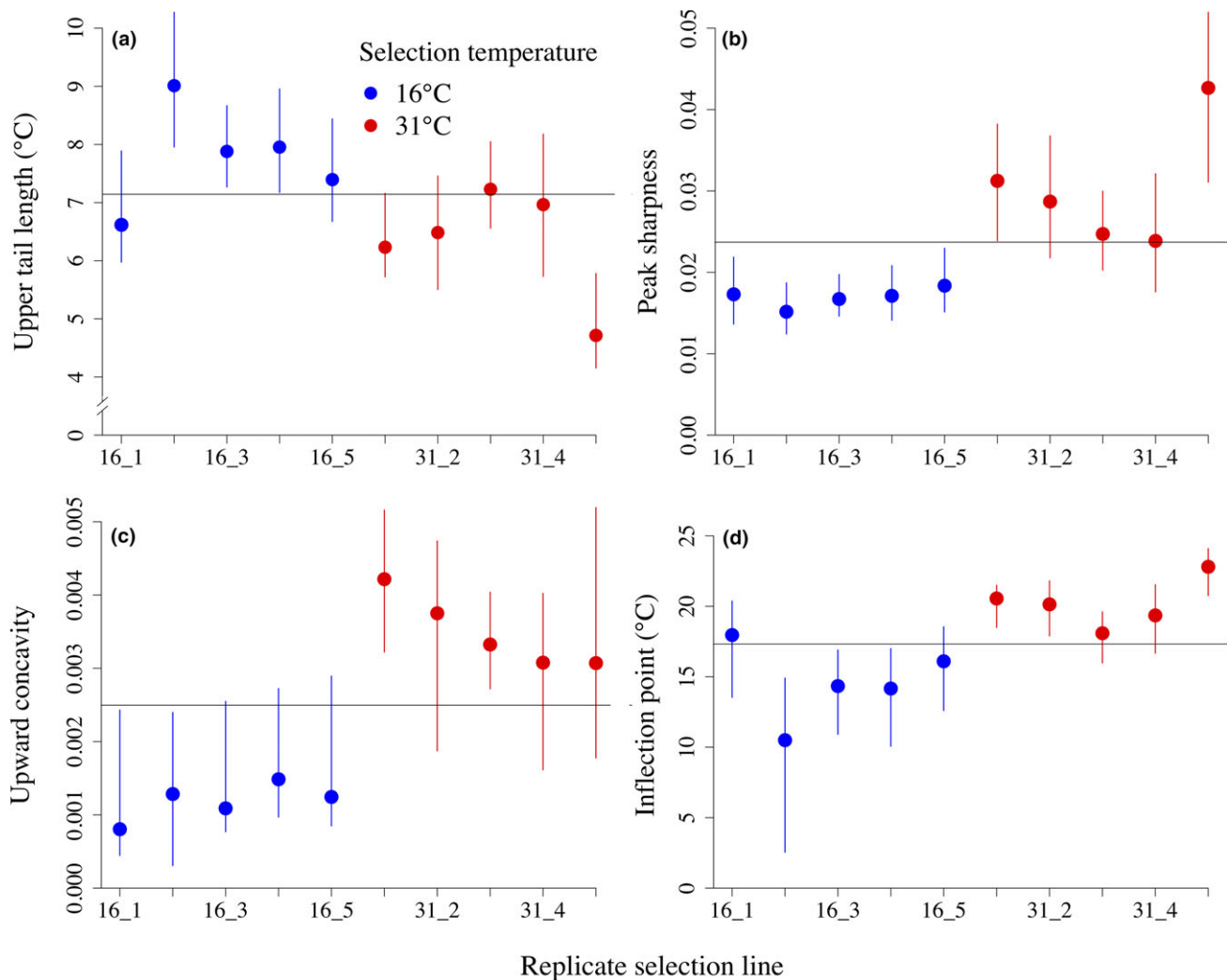


FIGURE 3 Thermal performance traits of 16°C- and 31°C-selected populations. II. (a) Upper tail lengths ($CT_{\max} - T_{\text{opt}}$) derived numerically from double-exponential curves ($n = 1,000$ bootstraps). (b) Peak sharpness of double-exponential curves. Sharpness is calculated as the negative of the second derivative of the double-exponential curve with respect to temperature at T_{opt} (larger values represent more negative gradients). (c) Upward concavity of double-exponential curves below T_{opt} , calculated as the maximum of the second derivative across $0 \leq T \leq T_{\text{opt}}$. (d) The inflection point below T_{opt} , where $\frac{\partial^2 \mu_{\max}}{\partial T^2} = 0$. Bars are 95% CI, estimated as the 2.5 to 97.5% quantiles of residual bootstrap distributions ($n = 1,000$)

was a significant *selection temperature* \times *assay temperature* interaction effect on μ_{\max} estimates derived from Monod fits ($F_{1,16} = 10.79$, $p = 0.0047$; Supporting information Table S3; Supporting information Figure S4; Supporting information Figure S5). A trade-off between the maximum growth rate and nitrate growth affinity was apparent in the 16°C-selected lines (Deming regression \pm 95% CI: slope = -0.098 ± 0.075 ; intercept = 0.11 ± 0.074) but was not statistically significant in the 31°C-selected lines (slope = -0.21 ± 0.35 ; intercept = 0.24 ± 0.61), with replicates pooled across assay temperatures (Figure 4).

4 | DISCUSSION

Evidence that phytoplankton can evolve rapidly in response to environmental change is mounting (Collins & Bell, 2004; Hutchins et al.,

2015; Listmann et al., 2016), but the response even to a single, directional selection pressure can be multifaceted (Hutchins et al., 2015; Low-Décarie, Jewell, Fussmann, & Bell, 2013; Schlüter et al., 2014). We showed that adaptation to different temperatures not only changes the growth rate at the selection temperature but also significantly alters the shape of the whole thermal reaction norm, a function-valued trait. The changes included shifts of a critical temperature trait, T_{opt} , and changes in the slope and curvature of the thermal reaction norm. Adaptation to high temperature resulted in a growth rate decline at low temperatures (a performance trade-off). In contrast, despite some evidence for a trade-off between maximum growth rate (μ_{\max}) and competitive ability for nitrate (indicated by nitrate growth affinity, a_{NO_3}) in the 16°C-selected populations (Figure 4), evolution of high μ_{\max} did not consistently lead to a reduction in a_{NO_3} under the selection conditions in this study. Pleiotropic

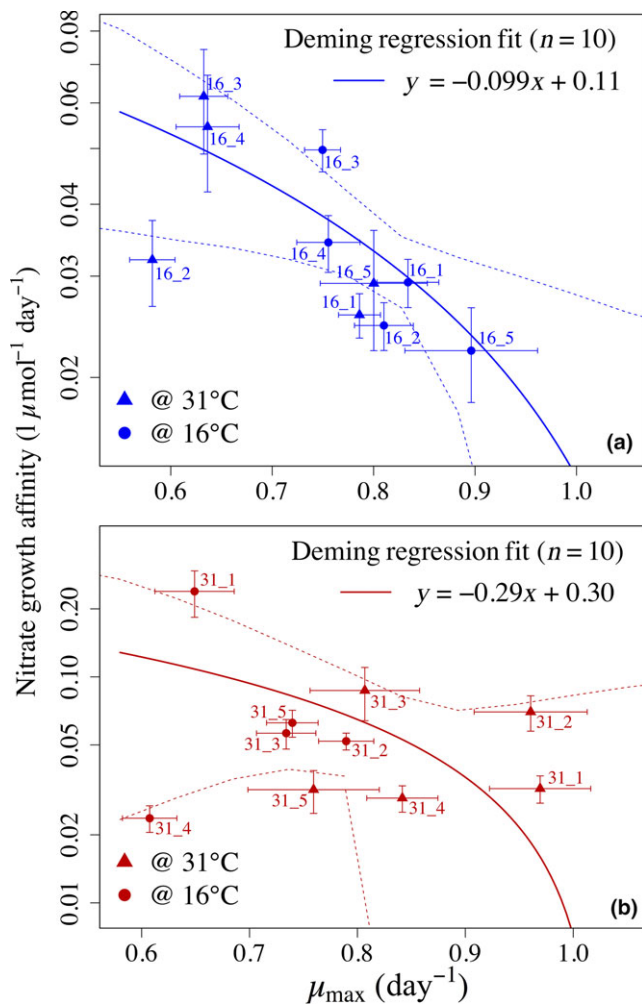


FIGURE 4 Deming regression plots for nitrate growth affinity (a_{NO_3}) versus maximum growth rate (μ_{max}). Traits are estimated from maximum likelihood fits of the Monod equation to nitrate-dependent growth assay data. (a) 16°C-selected lines; (b) 31°C-selected lines. Curves are Deming regression fits. Confidence bands are calculated using a residual bootstrap of the regression fit ($n = 1,000$ bootstraps), and account for uncertainty in each point, taken from Monod equation fits. All points are displayed with ± 1 SEM from Monod parameter estimates. Note that y-axis scales differ between panels, and that y-axes in both panels are on a log scale, resulting in apparent curvature of linear fits

effects (Elena & Lenski, 2003) or resource allocation or acquisition trade-offs (Angilletta et al., 2003; Gilchrist, 1995) associated with nitrogen acquisition or utilization were apparently minimal or absent.

While we cannot be certain that selection was stronger and the degree of evolution greater in warm- versus cold-adapted populations or vice versa (we lack a common, ancestral thermal reaction norm for our *T. pseudonana* populations, as assays on ancestral strains were conducted in ESAW medium preventing direct comparisons to contemporary strains), we can confidently infer evolutionary divergence between 16°C- and 31°C-adapted populations from their measured derived traits (as in Huey, Partridge, & Fowler, 1991). Selection at 31°C, well above the previously recorded T_{opt} for

T. pseudonana (Boyd et al., 2013) led to a divergence in T_{opt} of $\sim 2^\circ\text{C}$, on average. Furthermore, at the conclusion of the evolution experiment, T_{opt} of 16°C-selected were comparable to previously observed T_{opt} for *T. pseudonana* (Boyd et al., 2013), suggesting that the divergence between 16°C- and 31°C-selected populations was primarily driven by evolution of higher T_{opt} in 31°C-selected populations. Concurrent with this shift, the maximum growth rate at T_{opt} (μ_{opt}) diverged by $\sim 0.1/\text{day}$ ("vertical shift" [Izem & Kingsolver, 2005]) notably, the vertical shift also coincided with a narrowing of the region of the thermal reaction norm immediately adjacent to T_{opt} in 31°C-selected lines, such that less of the curve was in the near-optimal range (Figure 1). All strains but one (replicate line 16_1) met both the "local versus foreign" and "home versus away" criteria for demonstrating local adaptation at both 16°C and 31°C (Blanquart et al., 2013; Kawecki & Ebert, 2004).

The results suggest that the variation in *T. pseudonana*'s thermal reaction norm caused by thermal adaptation led to (or was driven by) a number of trade-offs. First, while we could not precisely estimate CT_{min} or the thermal niche width, the performance trade-off resulting from selection at 16°C versus at 31°C, combined with change in T_{opt} (and a suggestion of change in CT_{max} , though this was nonsignificant) suggest some horizontal shift in the thermal reaction norm (Izem & Kingsolver, 2005; Kingsolver, 2009), as previously observed in bacteriophages (Knies et al., 2006) and the marine coccolithophore *Emiliana huxleyi* (Listmann et al., 2016)—however, this trade-off may also result from thermal reaction norms of 31°C-selected populations becoming more concave-up below T_{opt} , and from changes in their higher inflection points (Figure 3). In addition, both temperature "generalist-specialist" and resource allocation trade-offs were apparent (Angilletta et al., 2003; Gilchrist, 1995), leading to a "diagonal stretch" in thermal reaction norms toward the upper right. The higher, sharper peaks and compressed upper tails in the thermal reaction norm of 31°C-selected lines, accompanied by a reduction in fitness at 16°C, suggest greater specialization for growth at high temperatures in 31°C-selected lines and less specialization in general in 16°C-selected lines.

We hypothesized that the evolutionary changes in the shape of the thermal reaction norm in response to selection at high temperature may be explained by increased allocation to cellular repair machinery. To test the plausibility of this hypothesis, we modified Equation 1 to include differential allocation to repair machinery, which provides the benefit of high-temperature tolerance while incurring the costs of increased nutrient requirements and reduced growth. In high-temperature adapted species, the thermodynamically predicted temperature of maximum enzyme stability falls well below the statistically fit T_{opt} (Corkrey et al., 2014; Ratkowsky et al., 2005), suggesting that it is rapid repair, rather than enhanced stability of enzymes that allows for positive growth at very high temperatures. The trade-off in the following model assumes lack of plasticity in resource allocation to enzyme repair at high temperatures versus reproduction across temperatures (Angilletta et al., 2003).

$$f(T) = b_1 e^{b_2 T} - d_1 e^{d_2 T} - d_0, \quad (3)$$

$$d_1 = \frac{d_1'}{p} \quad (4)$$

$$q = q_0 + q_1 p \quad (5)$$

$$b_1 = \frac{b_1'}{q}, \quad (6)$$

Here, the exponential mortality term ($d_1 e^{d_2 T}$ in [3.1]) is weighted inversely by p , which represents investment in protection from heat-induced denaturation of enzymes (or the induction of repair enzyme activity) (3.2); q is the nutrient content of a cell (quota), which is linearly related to p (3.3). Thus, as investment in protection and repair increases, temperature-dependent mortality decreases. However, temperature-dependent birth is also negatively affected as resources are diverted from reproduction and allocated to protection (3.4). The modified double-exponential model can produce changes in the curvature of the thermal reaction norm similar to those observed in our *T. pseudonana* selection experiment (Figure 5). The model predicts that peak sharpness at T_{opt} , upward concavity below T_{opt} , and the location of the inflection point are all positive, saturating functions of p (Supporting information Figure S7).

There are two observed results that this model does not predict, though the second follows from the first. First, the model predicts comparable evolutionary lability of T_{opt} and CT_{max} (Supporting information Figure S7a), while in experiments, the difference in CT_{max} between 31°C- and 16°C-selected populations was not statistically significant. Evolution of CT_{max} may thus be constrained by other physiological barriers not incorporated in the model. Second, the model predicts that upper tail length is a positive, saturating function

of p , only changing appreciably where $p < 0.2$ (Supporting information Figure S7b). In contrast, the upper tails of our experimentally derived thermal reaction norms were more compressed in 31°C-selected lines, compared to 16°C-selected lines (Figure 3a), and ranged in width from ~4°C to ~9°C. Although evolution of CT_{max} in response to temperature selection has been observed in the bacterium *Escherichia coli* (Mongold, Bennett, & Lenski, 1996) and in the marine coccolithophore *Emiliana huxleyi* (Listmann et al., 2016), the lack of significant change in CT_{max} relative to T_{opt} in this study suggest that, at least in *T. pseudonana*, T_{opt} is more evolutionarily labile than CT_{max} (Araújo et al., 2013). However, the vast diversity in CT_{max} in nature (Corkrey et al., 2014; Thomas et al., 2012), and in diatoms in particular (Thomas, Kremer, & Litchman, 2016), indicates that such constraints are not evolutionarily insurmountable. It is possible that on timescales relevant to the current rate of increase of global sea surface temperature, constraints on evolution of a higher CT_{max} may cause regional extinctions, contributing to diversity loss, especially at low latitudes (Thomas et al., 2012).

The trade-off between μ_{max} and resource affinities may be a general trend in nature (Grover, 1991; Klausmeier et al., 2004), but the overall weak and idiosyncratic response of nitrate affinity to temperature selection in our experiment may imply that temperature selection acted most strongly on systems other than those involved in nitrate uptake and utilization. However, the apparent trade-off in 16°C-selected lines but not in 31°C-selected lines (Figure 4) suggests that thermal adaptation to high temperature may make the trade-off weaker. In the absence of persistent nutrient limitation (and thus any selection for enhanced nutrient competitive ability, as was likely the case here), selection at a constant temperature should favor high μ_{max} at that temperature. If a $\mu_{\text{max}}-a_{\text{NO}_3}$ trade-off were driven by temperature selection, we would predict a concomitant decrease in competitive ability for nitrate, but changes in a_{NO_3} in response to temperature selection were not consistent and did not suggest a trade-off driven by temperature selection. Here, μ_{max} at both “home” and “away” temperatures changed predictably in response to temperature selection, but a_{NO_3} did not. The absence of an assay temperature effect on a_{NO_3} suggests that any $\mu_{\text{max}}-a_{\text{NO}_3}$ trade-off does not depend on the temperature environment in the short term, at least within the temperature range explored here, and that strong selection acted on μ_{max} alone, without pleiotropic effects on nitrate competitive ability in most replicates.

Thermal adaptation in the ocean would frequently occur under nitrogen limitation, at least in the temperate ocean where *T. pseudonana* is commonly found (Fong, 2008), and may thus produce changes in nitrogen affinities different from those we observed here. Therefore, we suggest that future temperature selection experiments should also account for nutrient limitation to reflect possible climate change scenarios in natural systems.

Evolution experiments are essential to enhancing our understanding of the effects of climate change on marine and freshwater food webs. Arguably, phytoplankton are among the highest payoff organisms upon which we can conduct evolution experiments: they offer a unique combination of potential for rapid evolutionary

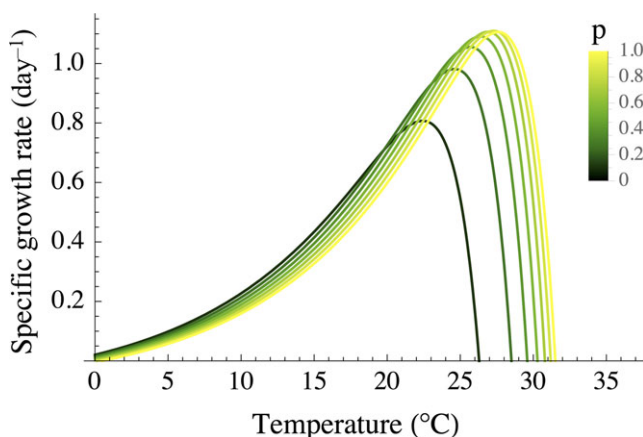


FIGURE 5 The modified double-exponential model with allocation to thermal protection (p) ranging from 0.1 to 1. Other parameter values are as follows: $b_1 = 0.124$, $b_2 = 0.1$, $d_0 = 0.1$, $d_1 = 3.059 \times 10^{-7}$, $d_2 = 0.5$, $q_0 = 1$, $q_1 = 0.3$

responses to environmental change, tractability as experimental subjects, and global ecological importance (Reusch & Boyd, 2013). Eco-evolutionary responses to changes in temperature, ocean acidity, nutrient limitation and other environmental factors are complex, and are made more complex by interactions among these factors. Single-stressor evolution experiments are a valuable first step, but future evolution experiments must account for interactive effects of multiple stressors (e.g., temperature and nitrate limitation).

ACKNOWLEDGEMENTS

We thank Mridul Thomas for culturing tips and conceptual input. This work would have been impossible without the support of our technicians at Kellogg Biological Station, Allyson Hutchins and Pamela Woodruff, and our NSF Research Experience for Teachers (RET) mentee, Connie High. DRO was in part supported by the National Science Foundation Graduate Research Fellowship, and by the Kellogg Biological Station Undergraduate Mentor Fellowship. This work was funded by NSF Grants OCE 0928819 and 1638958 to EL and CAK.

AUTHOR CONTRIBUTIONS

DRO designed experiments and conducted experiments, statistical analyses, and model analyses, and wrote the manuscript. CRH assisted in experimental design and conducted many of the experiments under the guidance of DRO. ECJ assisted with experiments and modeling. CTK developed the alternative parameterization of the double-exponential model and consulted on its implementation in the manuscript. CAK designed the double-exponential model and consulted on its analysis, and edited the manuscript. EL conceived the original experimental plan, consulted on and provided material support for all experiments, analysis and writing, and heavily edited the manuscript.

ORCID

Daniel R. O'Donnell  <http://orcid.org/0000-0003-0452-2888>

REFERENCES

- Angilletta, M. J., Wilson, R. S., Navas, C. A., & James, R. S. (2003). Trade-offs and the evolution of thermal reaction norms. *Trends in Ecology and Evolution*, 18, 234–240. [https://doi.org/10.1016/S0169-5347\(03\)00087-9](https://doi.org/10.1016/S0169-5347(03)00087-9)
- Araújo, M., Ferri-Yáñez, F., Bozinovic, F., Marquet, P. A., Valladares, F., & Chown, S. L. (2013). Heat freezes niche evolution. *Ecology Letters*, 16, 1206–1219. <https://doi.org/10.1111/ele.12155>
- Baker, K. G., Robinson, C. M., Radford, D. T., McInnes, A. S., Evenhuis, C., & Doblin, M. A. (2016). Thermal performance curves of functional traits aid understanding of thermally induced changes in diatom-mediated biogeochemical fluxes. *Frontiers in Marine Science*, 3, 1–14.
- Bell, G. (2013). Evolutionary rescue and the limits of adaptation. *Philosophical Transactions of the Royal Society of London B: Biological Sciences*, 368, 20120080.
- Bennett, A. F., & Lenski, R. E. (1993). Evolutionary adaptation to temperature II. Thermal niches of experimental lines of *Escherichia coli*. *Evolution*, 47, 1–12. <https://doi.org/10.1111/j.1558-5646.1993.tb01194.x>
- Blanquart, F., Kaltz, O., Nuismer, S. L., & Gandon, S. (2013). A practical guide to measuring local adaptation. *Ecology Letters*, 16, 1195–1205. <https://doi.org/10.1111/ele.12150>
- Bolker, B., & R Core Team (2017). *bbmle: tools for general maximum likelihood estimation*. R package version 1.0.19. <https://cran.r-project.org/web/packages/bbmle/index.html>
- Boyce, D. G., Lewis, M. R., & Worm, B. (2010). Global phytoplankton decline over the past century. *Nature*, 466, 591–596. <https://doi.org/10.1038/nature09268>
- Boyd, P. W., Rynearson, T. A., Armstrong, E. A., Fu, F., Hayashi, K., Hu, Z., ... Thomas, M. K. (2013). Marine phytoplankton temperature versus growth responses from polar to tropical waters – outcome of a scientific community-wide study. *PLoS One*, 8, e63091. <https://doi.org/10.1371/journal.pone.0063091>
- Bradford, M. A. (2013). Thermal adaptation of decomposer communities in warming soils. *Frontiers in Microbiology*, 4, 1–16.
- Collins, S., & Bell, G. (2004). Phenotypic consequences of 1,000 generations of selection at elevated CO₂ in a green alga. *Nature*, 431, 566–569. <https://doi.org/10.1038/nature02945>
- Corkrey, R., McMeekin, T. A., Bowman, J. P., Ratkowsky, D. A., Olley, J., & Ross, T. (2014). Protein thermodynamics can be predicted directly from biological growth rates. *PLoS One*, 9, e96100. <https://doi.org/10.1371/journal.pone.0096100>
- Crawford, K. J., Raven, J. A., Wheeler, G. L., Baxter, E. J., & Joint, I. (2011). The response of *Thalassiosira pseudonana* to long-term exposure to increased CO₂ and decreased pH. *PLoS One*, 6, e26695. <https://doi.org/10.1371/journal.pone.0026695>
- Elena, S. F., & Lenski, R. E. (2003). Evolution experiments with microorganisms: The dynamics and genetic bases of adaptation. *Nature Reviews Genetics*, 4, 457–469. <https://doi.org/10.1038/nrg1088>
- Field, C. B., Behrenfeld, M. J., Randerson, J. T., & Falkowski, P. G. (1998). Primary production of the biosphere: Integrating terrestrial and oceanic components. *Science*, 281, 237–240. <https://doi.org/10.1126/science.281.5374.237>
- Fong, P. (2008). Macroalgal-dominated ecosystems. In D. G. Capone, D. A. Bronk, M. R. Mulholland, & E. J. Carpenter (Eds.), *Nitrogen in the marine environment* (2nd ed., pp. 917–947). Cambridge, MA: Academic Press (Elsevier). <https://doi.org/10.1016/B978-0-12-372522-6.00020-7>
- Gilchrist, G. W. (1995). Specialists and generalists in changing environments. I. Fitness landscapes of thermal sensitivity. *The American Naturalist*, 146, 252–270. <https://doi.org/10.1086/285797>
- Gomulkiewicz, R., & Holt, R. D. (1995). When does evolution by natural selection prevent extinction? *Evolution*, 49, 201–207. <https://doi.org/10.1111/j.1558-5646.1995.tb05971.x>
- Grover, J. P. (1991). Resource competition in a variable environment: Phytoplankton growing according to the variable-internal-stores model. *The American Naturalist*, 138, 811–835. <https://doi.org/10.1086/285254>
- Guillard, R., & Hargraves, P. (1993). *Stichochrysis immobilis* is a diatom, not a chrysophyte. *Phycologia*, 32, 234–236. <https://doi.org/10.2216/i0031-8884-32-3-234.1>
- Harrison, P., Waters, R., & Taylor, F. (1980). A broad spectrum artificial seawater medium for coastal and open ocean phytoplankton. *Journal of Phycology*, 16, 28–35. <https://doi.org/10.1111/j.1529-8817.1980.tb00724.x>
- Healy, F. P. (1980). Slope of the Monod equation as an indicator of advantage in nutrient competition. *Microbial Ecology*, 5, 281–286. <https://doi.org/10.1007/BF02020335>
- Hinners, J., Kremp, A., & Hense, I. (2017). Evolution in temperature-dependent phytoplankton traits revealed from a sediment archive: Do reaction norms tell the whole story? *Proceedings of the Royal Society B*, 284, 20171888. <https://doi.org/10.1098/rspb.2017.1888>

- Hoffmann, A. A., & Sgrò, C. M. (2011). Climate change and evolutionary adaptation. *Nature*, 470, 479–485. <https://doi.org/10.1038/nature09670>
- Huey, R. B., Partridge, L., & Fowler, K. (1991). Thermal Sensitivity of *Drosophila melanogaster* responds rapidly to laboratory natural selection. *Evolution*, 45, 751–756. <https://doi.org/10.1111/j.1558-5646.1991.tb04343.x>
- Hutchins, D. A., Walworth, N. G., Webb, E. A., Saito, M. A., Moran, D., McIlvin, M. R., ... Fu, F.-X. (2015). Irreversibly increased nitrogen fixation in *Trichodesmium* experimentally adapted to elevated carbon dioxide. *Nature Communications*, 6, 8155. <https://doi.org/10.1038/ncomms9155>
- Izem, R., & Kingsolver, J. G. (2005). Variation in continuous reaction norms: Quantifying directions of biological interest. *The American Naturalist*, 166, 277–289. <https://doi.org/10.1086/431314>
- Jiang, H., & Gao, K. (2004). Effects of lowering temperature during culture on the production of polyunsaturated fatty acids in the marine diatom *Phaeodactylum tricornutum* (Bacillariophyceae). *Journal of Phycology*, 40, 651–654. [https://doi.org/10.1111/\(ISSN\)1529-8817](https://doi.org/10.1111/(ISSN)1529-8817)
- Jin, P., Gao, K., & Beardall, J. (2013). Evolutionary responses of a coccolithophorid *Gephyrocapsa oceanica* to ocean acidification. *Evolution*, 67, 1869–1878. <https://doi.org/10.1111/evo.12112>
- Kawecki, T. J., & Ebert, D. (2004). Conceptual issues in local adaptation. *Ecology Letters*, 7, 1225–1241. <https://doi.org/10.1111/j.1461-0248.2004.00684.x>
- Kingsolver, J. G. (2009). The well-temperated biologist. *The American Naturalist*, 174, 755–768.
- Kingsolver, J. G., Gomulkiewicz, R., & Carter, P. A. (2001). Variation, selection and evolution of function-valued traits. *Genetica*, 112, 87–104. <https://doi.org/10.1023/A:1013323318612>
- Klausmeier, C. A., Litchman, E., Daufresne, T., & Levin, S. A. (2004). Optimal nitrogen-to-phosphorus stoichiometry of phytoplankton. *Nature*, 429, 171–174. <https://doi.org/10.1038/nature02454>
- Knies, J. L., Izem, R., Supler, K. L., Kingsolver, J. G., & Burch, C. L. (2006). The genetic basis of thermal reaction norm evolution in lab and natural phage populations. *PLoS Biology*, 4, e201. <https://doi.org/10.1371/journal.pbio.0040201>
- Kutcherov, D. (2016). Thermal reaction norms can surmount evolutionary constraints: Comparative evidence across leaf beetle species. *Ecology and Evolution*, 6, 4670–4683. <https://doi.org/10.1002/ece3.2231>
- Listmann, L., LeRoch, M., Schlüter, L., Thomas, M. K., & Reusch, T. B. H. (2016). Swift thermal reaction norm evolution in a key marine phytoplankton species. *Evolutionary Applications*, 9, 1156–1164. <https://doi.org/10.1111/eva.12362>
- Litchman, E., Edwards, K., Klausmeier, C. A., & Thomas, M. (2012). Phytoplankton niches, traits and eco-evolutionary responses to global environmental change. *Marine Ecology Progress Series*, 470, 235–248. <https://doi.org/10.3354/meps09912>
- Litchman, E., Klausmeier, C. A., Schofield, O. M., & Falkowski, P. G. (2007). The role of functional traits and tradeoffs in structuring phytoplankton communities: Scaling from cellular to ecosystem level. *Ecology Letters*, 10, 1170–1181. <https://doi.org/10.1111/j.1461-0248.2007.01117.x>
- Logan, J. A., Wollkind, D. J., Hoyt, S. C., & Tanigoshi, L. K. (1976). An analytical model for description of temperature dependent rate phenomena in arthropods. *Environmental Entomology*, 5, 1133–1140. <https://doi.org/10.1093/ee/5.6.1133>
- Lohbeck, K. T., Riebesell, U., & Reusch, T. B. H. (2012). Adaptive evolution of a key phytoplankton species to ocean acidification. *Nature Geosciences*, 5, 346–351. <https://doi.org/10.1038/ngeo1441>
- Low-Décarie, E., Jewell, M. D., Fussmann, G. F., & Bell, G. (2013). Long-term culture at elevated atmospheric CO₂ fails to evoke specific adaptation in seven freshwater phytoplankton species. *Proceedings of the Royal Society B*, 280, 20122598. <https://doi.org/10.1098/rspb.2012.2598>
- Manuilova, E., Schuetzenmeister, A., & Model, F. (2014). mcr: Method comparison regression. R package version 1.2.1. <https://cran.r-project.org/package=mcr>
- Martiny, A. C., Ma, L., Mougnot, C., Chandler, J. W., & Zinser, E. R. (2016). Interactions between thermal acclimation, growth rate, and phylogeny influence *Prochlorococcus* elemental stoichiometry. *PLoS One*, 11, e0168291. <https://doi.org/10.1371/journal.pone.0168291>
- Mongold, J. A., Bennett, A. F., & Lenski, R. E. (1996). Evolutionary adaptation to temperature. IV. Adaptation of *Escherichia coli* at a niche boundary. *Evolution*, 50, 35–43. <https://doi.org/10.1111/j.1558-5646.1996.tb04470.x>
- Monod, J. (1949). The growth of bacterial cultures. *Annual Reviews in Microbiology*, 3, 371–394. <https://doi.org/10.1146/annurev.mi.03.100149.002103>
- Nedwell, D. (1999). Effect of low temperature on microbial growth: Lowered affinity for substrates limits growth at low temperature. *FEMS Microbiology and Ecology*, 30, 101–111. <https://doi.org/10.1111/j.1574-6941.1999.tb00639.x>
- Nelson, D. M., Tréguer, P., Brzezinski, M. A., Leynaert, A., & Quéguiner, B. (1995). Production and dissolution of biogenic silica in the ocean: Revised global estimates, comparison with regional data and relationship to biogenic sedimentation. *Global Biogeochemical Cycles*, 9, 359–372. <https://doi.org/10.1029/95GB01070>
- Neori, A., Vernet, M., Holm-Hansen, O., & Haxo, F. T. (1986). Relationship between action spectra for chlorophyll *a* fluorescence and photosynthetic O₂ evolution in algae. *Journal of Plankton Research*, 8, 537–548. <https://doi.org/10.1093/plankt/8.3.537>
- Padfield, D., Yvon-Durocher, G., Buckling, A., Jennings, S., & Yvon-Durocher, G. (2015). Rapid evolution of metabolic traits explains thermal adaptation in phytoplankton. *Ecology Letters*, 19, 133–142.
- Ratkowsky, D. A., Olley, J., & Ross, T. (2005). Unifying temperature effects on the growth rate of bacteria and the stability of globular proteins. *Journal of Theoretical Biology*, 233, 351–362. <https://doi.org/10.1016/j.jtbi.2004.10.016>
- Redfield, A. C. (1958). The biological control of chemical factors in the environment. *American Scientist*, 46, 205–221.
- Reusch, T. B. H., & Boyd, P. W. (2013). Experimental evolution meets marine phytoplankton. *Evolution*, 67, 1849–1859. <https://doi.org/10.1111/evo.12035>
- Rowan, R. (2004). Thermal adaptation in reef coral symbionts. *Nature*, 430, 742. <https://doi.org/10.1038/430742a>
- Schaum, C.-E., Barton, S., Bestion, E., Buckling, A., Garcia-Carreras, B., Lopez, P., ... Yvon-Durocher, G. (2017). Adaptation of phytoplankton to a decade of experimental warming linked to increased photosynthesis. *Nature Ecology Evolution*, 1, 0094. <https://doi.org/10.1038/s41559-017-0094>
- Schiffers, K., Bourne, E. C., Lavergne, S., Thuiller, W., & Travis, J. M. J. (2013). Limited evolutionary rescue of locally adapted populations facing climate change. *Philosophical Transactions of the Royal Society of London B: Biological Sciences*, 368, 20120083.
- Schlüter, L., Lohbeck, K. T., Gutowska, M. A., Gröger, J. P., Riebesell, U., & Reusch, T. B. H. (2014). Adaptation of a globally important coccolithophore to ocean warming and acidification. *Nature Climate Change*, 4, 1024–1030. <https://doi.org/10.1038/nclimate2379>
- Schoener, T. W. (2011). The newest synthesis: Understanding the interplay of evolutionary and ecological dynamics. *Science*, 331, 426–429. <https://doi.org/10.1126/science.1193954>
- Thomas, M. K., Aranguren-Gassis, M., Kremer, C. T., Gould, M. R., Anderson, K., Klausmeier, C. A., & Litchman, E. (2017). Temperature-nutrient interactions exacerbate sensitivity to warming in phytoplankton. *Global Change Biology*, 23, 3269–3280. <https://doi.org/10.1111/gcb.13641>
- Thomas, M. K., Kremer, C. T., Klausmeier, C. A., & Litchman, E. (2012). A global pattern of thermal adaptation in marine phytoplankton. *Science*, 338, 1085–1088. <https://doi.org/10.1126/science.1224836>

- Thomas, M. K., Kremer, C. T., & Litchman, E. (2016). Environment and evolutionary history determine phytoplankton temperature traits globally. *Global Ecology & Biogeography*, 25, 71–86.
- Thrane, J.-E., Hessen, D. O., & Anderson, T. (2017). Plasticity in algal stoichiometry: Experimental evidence of a temperature-induced shift in optimal supply N: P ratio. *Limnology and Oceanography*, 62, 1346–1354. <https://doi.org/10.1002/lno.10500>
- Tilman, D. A., Mattson, M., & Langer, S. (1981). Competition and nutrient kinetics along a temperature gradient: An experimental test of a mechanistic approach to niche theory. *Limnology and Oceanography*, 26, 1020–1033. <https://doi.org/10.4319/lo.1981.26.6.1020>
- Yvon-Durocher, G., Schaum, C.-E., & Trimmer, M. (2017). The temperature dependence of phytoplankton stoichiometry: Investigating the roles of species sorting and local adaptation. *Frontiers in Microbiology*, 8, 2003. <https://doi.org/10.3389/fmicb.2017.02003>

SUPPORTING INFORMATION

Additional supporting information may be found online in the Supporting Information section at the end of the article.

How to cite this article: O'Donnell DR, Hamman CR, Johnson EC, Kremer CT, Klausmeier CA, Litchman E. Rapid thermal adaptation in a marine diatom reveals constraints and trade-offs. *Glob Change Biol*. 2018;24:4554–4565. <https://doi.org/10.1111/gcb.14360>